

SCIENTIFIC REPORTS



OPEN

MicroRNAs as potential therapeutics to enhance chemosensitivity in advanced prostate cancer

Hui-Ming Lin^{1,2}, Iva Nikolic^{1,2,3}, Jessica Yang¹, Lesley Castillo¹, Niantao Deng^{1,2}, Chia-Ling Chan¹, Nicole K. Yeung¹, Eoin Dodson¹, Benjamin Elsworth¹, Calan Spielman¹, Brian Y. Lee^{1,9}, Zoe Boyer¹, Kaylene J. Simpson^{3,4}, Roger J. Daly^{5,6}, Lisa G. Horvath^{1,7,8} & Alexander Swarbrick^{1,2}

Docetaxel and cabazitaxel are taxane chemotherapy treatments for metastatic castration-resistant prostate cancer (CRPC). However, therapeutic resistance remains a major issue. MicroRNAs are short non-coding RNAs that can silence multiple genes, regulating several signalling pathways simultaneously. Therefore, synthetic microRNAs may have therapeutic potential in CRPC by regulating genes involved in taxane response and minimise compensatory mechanisms that cause taxane resistance. To identify microRNAs that can improve the efficacy of taxanes in CRPC, we performed a genome-wide screen of 1280 microRNAs in the CRPC cell lines PC3 and DU145 in combination with docetaxel or cabazitaxel treatment. Mimics of miR-217 and miR-181b-5p enhanced apoptosis significantly in PC3 cells in the presence of these taxanes. These mimics downregulated at least a thousand different transcripts, which were enriched for genes with cell proliferation and focal adhesion functions. Individual knockdown of a selection of 46 genes representing these transcripts resulted in toxic or taxane sensitisation effects, indicating that these genes may be mediating the effects of the microRNA mimics. A range of these genes are expressed in CRPC metastases, suggesting that these microRNA mimics may be functional in CRPC. With further development, these microRNA mimics may have therapeutic potential to improve taxane response in CRPC patients.

Prostate cancer is the second most frequently diagnosed cancer in men worldwide, and the third leading cause of male cancer death in developed countries¹. Despite the rise in new therapeutics for metastatic castration-resistant prostate cancer (CRPC) such as novel anti-androgens, radium-223 and PARP inhibitors^{2,3}, the taxanes docetaxel and cabazitaxel are the standard of care chemotherapy treatments for CRPC. For more than a decade, docetaxel has remained as the first line cytotoxic treatment for CRPC^{4,5}, and is now increasingly used in the metastatic castration-sensitive setting^{6,7}. However, only ~50% of patients respond to docetaxel, and responders eventually develop resistance^{4,5}. Cabazitaxel, a second-generation taxane, improves the survival of patients with docetaxel-resistant CRPC, but was not superior to docetaxel and thus remains as second line treatment with

¹Cancer Division, The Kinghorn Cancer Centre, Garvan Institute of Medical Research, Darlinghurst, New South Wales, 2010, Australia. ²St Vincent's Clinical School, UNSW Sydney, New South Wales, 2010, Australia. ³Victorian Centre for Functional Genomics, Peter MacCallum Cancer Centre, Melbourne, Victoria, 3000, Australia. ⁴The Sir Peter MacCallum Department of Oncology, University of Melbourne, Parkville, Victoria, 3000, Australia. ⁵Signalling Network Laboratory, Department of Biochemistry and Molecular Biology, Monash University, Clayton, Victoria, 3800, Australia. ⁶Cancer Program, Biomedicine Discovery Institute, Monash University, Clayton, Victoria, 3800, Australia. ⁷Medical Oncology, Chris O'Brien Lifehouse, Camperdown, New South Wales, 2050, Australia. ⁸Sydney Medical School, University of Sydney, Camperdown, New South Wales, 2050, Australia. ⁹Present address: Systems Oncology, Cancer Research UK Manchester Institute, The University of Manchester, Manchester, M20 4QL, United Kingdom. Correspondence and requests for materials should be addressed to L.G.H. (email: lisa.horvath@lh.org.au) or A.S. (email: a.swarbrick@garvan.org.au)

a response rate of ~60%^{8,9}. Overall, new therapeutic strategies are required to overcome taxane resistance and improve patient outcome.

MicroRNAs are short non-coding RNAs (~22 nucleotides) that regulate gene expression post-transcriptionally by forming an RNA-induced silencing complex which represses translation or degrades messenger RNA (mRNA)¹⁰. The complex is formed by a microRNA binding to the mRNA at a complementary 'seed' sequence on the 3' untranslated region of the mRNA, together with Argonaute proteins. Binding can occur with imperfect base pairing, thus a single microRNA can negatively regulate hundreds of different genes, and the mRNA of a single gene can be targeted by different microRNAs. Many microRNAs have tissue-specific expression¹¹, and over two thousand different microRNAs have been identified in humans¹².

The discovery of oncogenic and tumour-suppressor microRNAs, and the ability to manipulate cellular microRNA levels with modified oligonucleotides that mimic or inhibit their function has led to extensive research and development of microRNAs as therapeutics^{13,14}. By using a single microRNA to silence multiple genes, several signalling pathways can be regulated simultaneously and may thus minimise compensatory mechanisms that cause therapeutic resistance. Most microRNA-based therapeutics are still in the pre-clinical stages of research¹⁴. A few have completed Phase 1 or Phase 2 clinical trials with positive results, such as Miravirsen (miR-122 inhibitor) for hepatitis C viral infection¹⁵ and TagomiR (miR-16 mimic) for malignant pleural mesothelioma¹⁶.

A potential therapeutic application of microRNAs is to combine microRNA therapy with taxane chemotherapy to overcome chemoresistance. The availability of large libraries of microRNA mimics or inhibitors enables the use of genome-wide screens to identify microRNAs that can increase the sensitivity of cancer cells to a drug. This approach was commonly used with small-interfering RNA (siRNA) libraries to identify synthetic lethal genes¹⁷ but has been demonstrated with microRNA libraries. For example, Lam *et al.* identified 19 microRNAs that sensitised colorectal cancer cells to a BCL2 inhibitor from a screen of 810 microRNA mimics combined with the drug¹⁸.

To identify microRNAs that have therapeutic potential to overcome resistance to docetaxel and cabazitaxel in CRPC, we performed a genome-wide functional screen of CRPC cell lines PC3 and DU145, with microRNA mimics or inhibitors of 1280 microRNAs in combination with docetaxel or cabazitaxel treatment. MicroRNA mimics act as mature microRNAs, whereas microRNA inhibitors block the activity of endogenous microRNAs within a cell. The screen and the effects of the mimics/inhibitors on the cells without taxane treatment are described by Nikolic *et al.*¹⁹. Here, we present the findings from combining the screen with taxane treatment, where the effects and gene targets of two hits from the screen were further characterised.

Results

Identification of microRNAs that are taxane sensitisers. A high-throughput functional screen testing microRNA mimics or inhibitors of 1280 microRNAs in PC3 and DU145 cancer cell lines was performed to identify microRNA mimics or inhibitors that can increase the sensitivity of the cells to docetaxel or cabazitaxel. Non-targeting siRNA was used as the control for the microRNA mimics or inhibitors. The cells in the screen were treated with sub-optimal doses of docetaxel and cabazitaxel equivalent to an IC20 dose (drug concentration where response is reduced by 20%). Given that these doses of taxanes decreased cell viability by 20% in non-targeting control cells, we considered a microRNA mimic or inhibitor as a taxane sensitiser if it decreased cell viability by more than 20% with taxane treatment – i.e. viability of taxane-treated cells transfected with mimic or inhibitor is <80% of the viability of taxane-treated cells transfected with non-targeting control, and viability of vehicle-treated cells transfected with mimic or inhibitor is >80% of the viability of vehicle-treated cells transfected with non-targeting control.

These thresholds produced many hits among the microRNA mimics – 102 docetaxel sensitisers and 112 cabazitaxel sensitisers for PC3 cells, 61 docetaxel sensitisers and 49 cabazitaxel sensitisers for DU145 cells (Fig. 1a). Most of these hits only caused a modest effect with taxane treatment (70–80% viability), and only four reduced cell viability by more than 50% (Fig. 1a). None of the hits caused the same level of toxicity, with or without taxane treatment, as that of the positive control, PLK1 (polo-like kinase 1) siRNA, where the viability of PC3 and DU145 cells transfected with PLK1 siRNA was 22% and 6% respectively.

The number of microRNA inhibitors with taxane sensitisation effects were far less compared to the microRNA mimics – 71 docetaxel sensitisers and 37 cabazitaxel sensitisers for PC3 cells, 29 docetaxel sensitisers and 22 cabazitaxel sensitisers for DU145 cells (Supplementary Figure S1A). Unlike the microRNA mimics, none of the microRNA inhibitors reduced cell viability by more than 50% (Supplementary Figure S1B). The strongest taxane sensitisation effect by any of the inhibitors was 40% reduction in cell viability with cabazitaxel treatment, and 30% reduction in cell viability with docetaxel treatment.

The microRNA mimics with the strongest taxane sensitising effects – causing more than 50% cell death, were selected for further investigation. These consisted of miR-217, miR-181b-5p, miR-100-3p and miR-153 mimics (Fig. 1b). MiR-217, miR-181b-5p, and miR-100-3p increased the sensitivity of PC3 cells to either or both taxanes, whereas miR-153 increased the sensitivity of DU145 to cabazitaxel in the screen.

Effect of microRNA mimics on cell viability. Further validation with a range of taxane doses to generate dose response curves showed that miR-217 and miR-181b-5p mimics decreased the IC50 (drug concentration where response is reduced by 50%) of docetaxel or cabazitaxel, or enhanced the maximum response to the taxanes (lowest cell viability among the drug concentrations) (Fig. 2a). These mimics also modestly reduced cell number in the absence of taxanes, as cells transfected with the mimics grew more slowly than those transfected with the non-targeting control (Fig. 2b).

MiR-100-3p and miR-153 mimics also reduced cell number in transfected PC3 and DU145 cells in the absence of taxanes, but did not alter the IC50 or the maximum response of cabazitaxel in PC3 and DU145 respectively (Supplementary Figure S3). Therefore, miR-217 and miR-181b-5p were selected for further study as potential therapeutics.

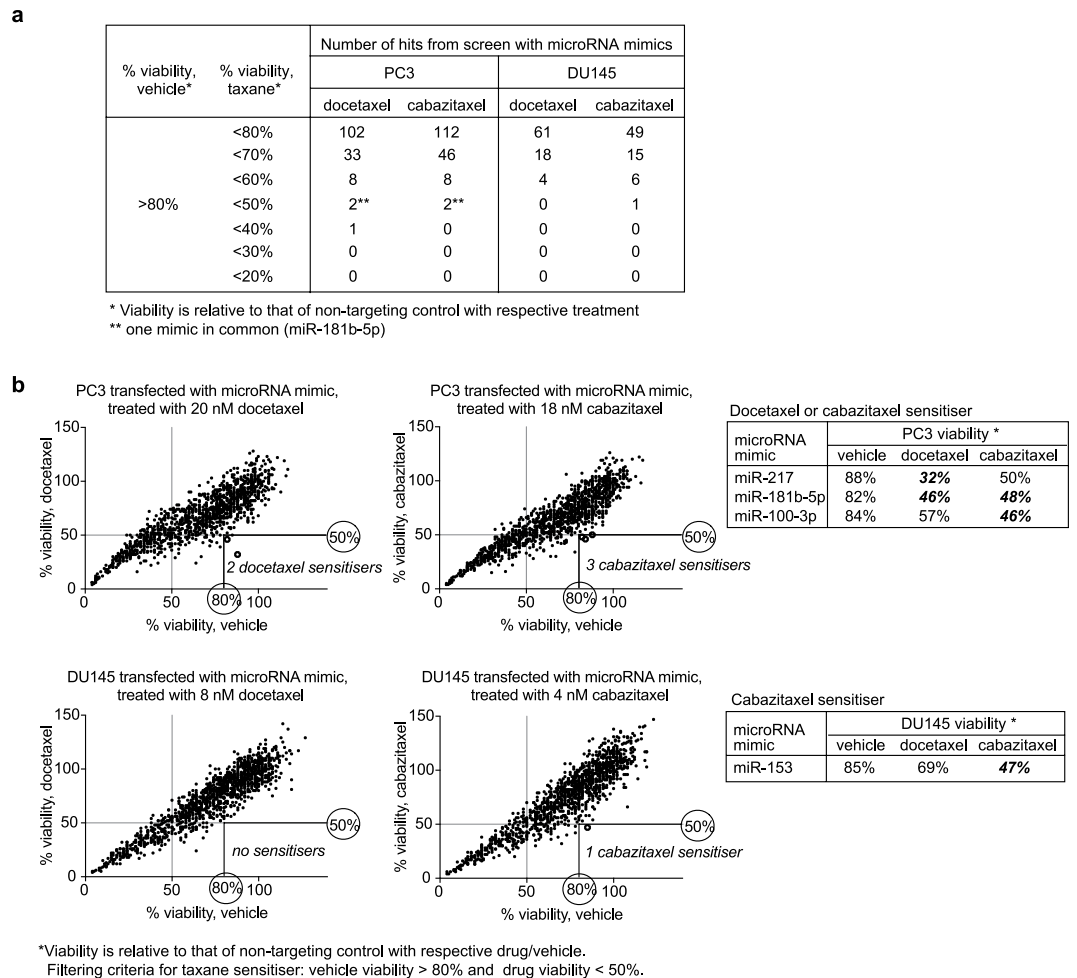


Figure 1. Identification of microRNA mimics with taxane sensitisation effects in PC3 and DU145 cell lines in a functional screen testing 1280 microRNA mimics individually in combination with docetaxel or cabazitaxel treatment: **(a)**. Number of hits at different thresholds of taxane sensitisation; **(b)**. Viability plots showing the thresholds for identifying the strongest taxane sensitisers in PC3 and DU145.

The slower growth rate of PC3 cells when transfected with the mimics may be partly attributed to enhanced apoptosis, as the percentage of apoptotic cells was significantly higher among cells transfected with the mimics compared to those transfected with the non-targeting control (Fig. 2c – 0 nM drug, $P < 0.05$). Addition of docetaxel or cabazitaxel significantly increased apoptosis in cells transfected with the mimics, compared to those transfected with non-targeting control (Fig. 2c – 10 nM docetaxel and 5 nM cabazitaxel, $P < 0.05$).

There were no significant differences in the percentage of cells in the cell cycle phases of G1, S, and G2-M for cells transfected with the mimics compared to those transfected with the non-targeting control, with or without taxane treatment (Fig. 2d). Docetaxel and cabazitaxel caused cell cycle arrest in the G2-M phase as expected, without any significant differences in cell numbers between mimics and non-targeting control (Fig. 2d, $P > 0.05$). These findings indicate that enhanced apoptosis by the mimics occurred through mechanisms that did not involve alterations to the taxanes' induction of G2-M cell cycle arrest.

The effects of miR-217 and miR181b-5p on cell viability were only specific to PC3 and not DU145, as these mimics did not alter the taxane dose response curves or enhanced apoptosis in DU145 cells (Supplementary Figure S4).

Genes regulated by microRNA mimics. To identify genes and pathways that were regulated by the microRNA mimics, RNA-sequencing was performed on PC3 cells transfected with miR-217 or miR-181b-5p mimics. Filtered reads were mapped to 27,718 genes. The number of transcripts significantly downregulated in cells transfected with miR-217 or miR-181b-5p mimics compared to non-targeting control were 1295 and 1355 respectively (adjusted $P < 0.05$), of which 402 (~30%) were in common. According to the microRNA target database TarBase (version 7)²⁰, 48 (4%) and 258 (19%) of the transcripts downregulated by miR-217 and miR-181b-5p mimics respectively were experimentally-supported targets. Our own database¹⁹ predicted that 490 (38%) and 518 (38%) of the transcripts downregulated by miR-217 and miR-181b-5p mimics respectively were direct targets of these mimics. The target predictions made by our database were the combined results from established target prediction algorithms by StarBase, MIRTarBase, TargetScan, DIANA and MIRDB¹⁹.

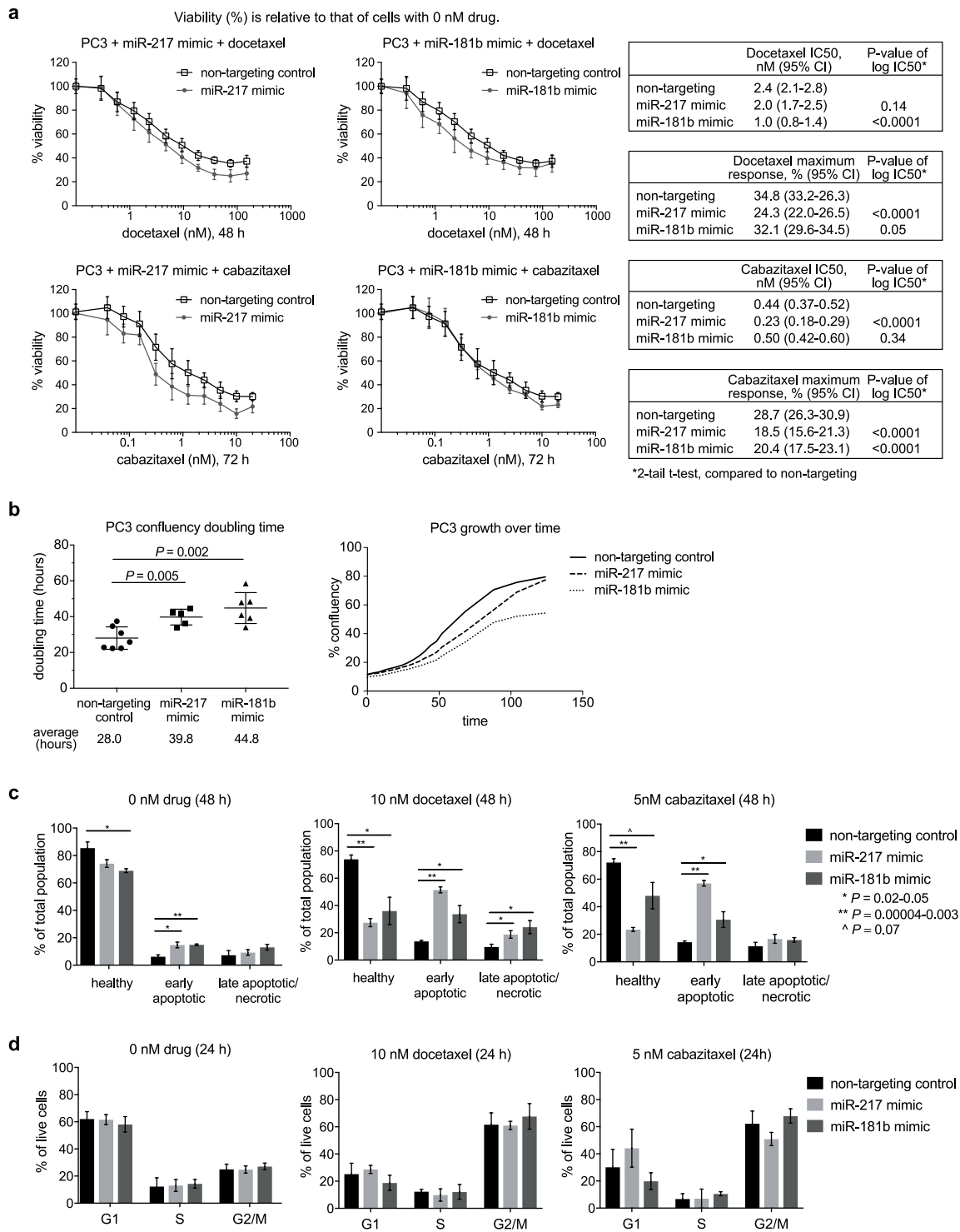
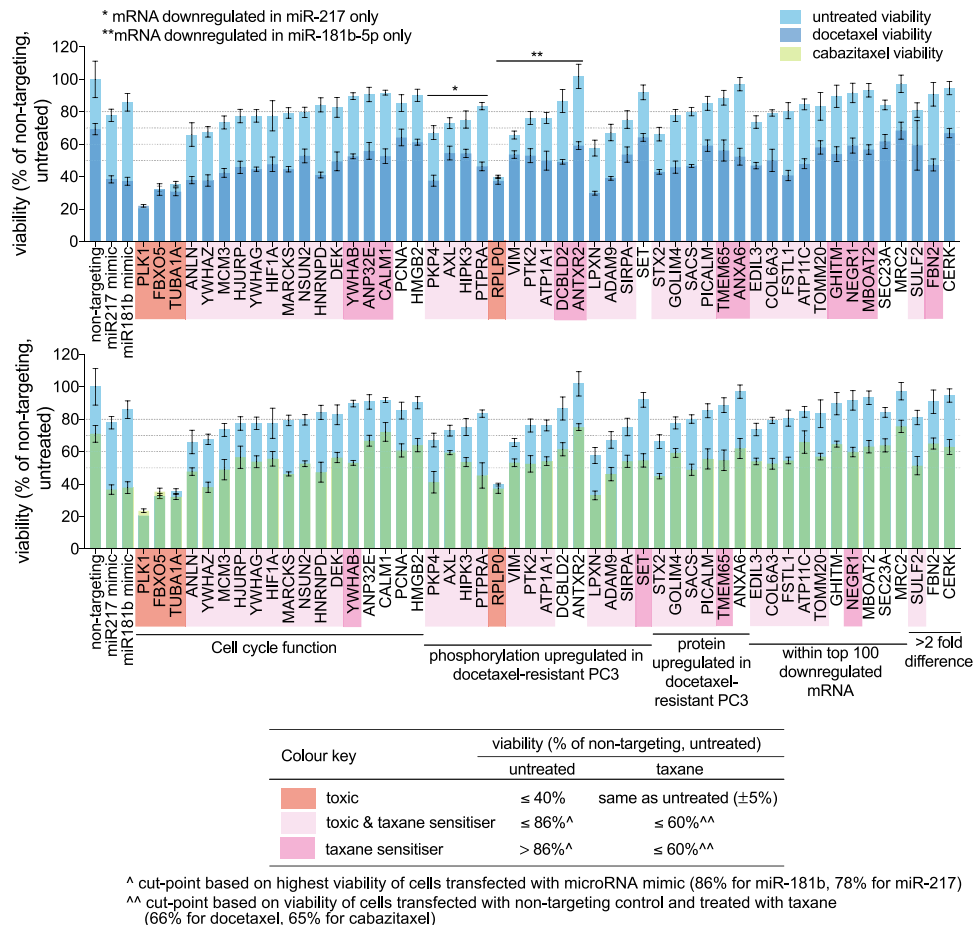


Figure 2. Assessment of cell viability, apoptosis, and cell cycle phases in PC3 cells transfected with miR-217 or miR-181b-5p mimic: **(a)**. Docetaxel and cabazitaxel dose response curves (mean \pm standard deviations of 3 experiments with 4 replicate samples each); **(b)**. Doubling times measured using IncuCyte ZOOM, and an example of growth curves from one of the experiments (single technical replicate per condition; other replicates shown in Supplementary Figure S2); **(c)**. Percentage of apoptotic cells, quantitated by flow cytometry with annexin-V-FITC and propidium iodide labelling (mean \pm standard deviations of 3 experiments); **(d)**. Percentage of cells in cell cycle phases, quantitated by flow cytometry with propidium iodide staining (mean \pm standard deviations of 3 experiments).

miR-217 mimic-transfected PC3 cells (1274 genes recognised by MSigDB)				
Top 10 Hallmark gene sets		Genes in gene set	Genes in overlap	P-value
1	E2F targets ^a	200	64	2.2×10^{-49}
2	G2M checkpoint ^a	200	61	1.0×10^{-45}
3	Mitotic spindle ^a	200	44	1.5×10^{-25}
4	Epithelial-mesenchymal-transition ^b	200	40	8.3×10^{-23}
5	MYC targets	200	38	6.5×10^{-21}
6	Estrogen response late	200	29	3.9×10^{-13}
7	DNA repair	150	25	6.7×10^{-13}
8	Apical junction	200	27	1.4×10^{-11}
9	Myogenesis	200	24	2.1×10^{-9}
10	UV response	144	20	3.6×10^{-9}
Top 10 KEGG gene sets		Genes in gene set	Genes in overlap	P-value
1	DNA replication ^a	36	15	1.3×10^{-14}
2	Cell cycle ^a	128	24	1.3×10^{-13}
3	Focal Adhesion ^b	201	28	2.7×10^{-12}
4	Nucleotide excision repair	44	13	1.3×10^{-10}
5	ECM receptor interaction ^b	84	16	1.2×10^{-9}
6	Pathways in cancer	328	31	3.9×10^{-9}
7	Mismatch repair	23	9	5.4×10^{-9}
8	Pathogenic E. Coli infection	59	13	6.7×10^{-9}
9	Ubiquitin mediated proteolysis	138	19	1.0×10^{-8}
10	Oocyte meiosis	114	17	1.8×10^{-8}
miR-181b-5p mimic-transfected PC3 cells (1337 genes recognised by MSigDB)				
Top 10 Hallmark gene sets		Genes in gene set	Genes in overlap	P-value
1	MYC targets	200	105	4.6×10^{-106}
2	G2M checkpoint ^a	200	76	2.0×10^{-63}
3	E2F targets ^a	200	72	3.6×10^{-58}
4	Mitotic spindle ^a	200	56	1.1×10^{-38}
5	MTORC1 signaling	200	56	1.1×10^{-38}
6	Oxidative phosphorylation	200	49	5.0×10^{-31}
7	Epithelial mesenchymal transition ^b	200	46	6.4×10^{-28}
8	Fatty acid metabolism	158	35	5.2×10^{-21}
9	Glycolysis	200	37	2.7×10^{-19}
10	Adipogenesis	200	31	3.4×10^{-14}
Top 10 KEGG gene sets		Genes in gene set	Genes in overlap	P-value
1	Ribosome	88	36	4.5×10^{-32}
2	Huntingtons disease	185	38	1.9×10^{-21}
3	Oocyte meiosis	114	30	1.7×10^{-20}
4	Spliceosome	128	31	5.5×10^{-20}
5	Cell cycle ^a	128	30	6.0×10^{-19}
6	Parkinsons disease	133	29	1.9×10^{-17}
7	Alzheimers disease	169	32	3.4×10^{-17}
8	Focal adhesion ^b	201	34	1.3×10^{-16}
9	Pathways in cancer	328	40	2.8×10^{-14}
10	Oxidative phosphorylation	135	25	1.6×10^{-13}

Table 1. Biological themes enriched among RNA transcripts downregulated by microRNA mimics, based on significant overlaps with gene sets from the Molecular Signatures Database (MSigDB). ^aCell proliferation theme. ^bFocal adhesion theme.

The Molecular Signatures Database²¹ was used to identify biological themes that were enriched among the downregulated transcripts, as these themes may provide insights into the function of the gene targets and hence the mechanism of the microRNA mimics. Several of the biological themes that were significantly enriched among the downregulated transcripts in cells transfected with either miR-217 or miR-181b-5p mimics were related to cell proliferation and focal adhesion (Table 1).



	Validated gene targets (Tarbase v.7)
miR-217	ATP11C, DEK, HIF1A
miR-181b-5p	ANP32E, DEK, FSTL1, GHITM, HMGB2, MBOAT2, PICALM, PTK2, RPLP0, TOMM20, YWHAB, YWHAG

Figure 3. Effects of siRNA knockdown of 51 gene targets of miR-217 or miR-181b-5p mimics on the docetaxel or cabazitaxel sensitivity of PC3 cells. Cells were treated with 10 nM docetaxel or 5 nM cabazitaxel after siRNA transfection. Barplots show viability of siRNA-transfected cells, with or without taxane treatment, relative to that of cells transfected with non-targeting siRNA control without taxane treatment. Datapoints are mean ± standard deviations of 4 replicate samples.

To determine if the downregulated transcripts mediate the taxane sensitisation effect of the microRNA mimics, siRNA SMARTpool knockdown of 51 genes individually in PC3 cells in combination with docetaxel or cabazitaxel treatment was performed with miR-217 and miR-181b mimics as positive controls (full names listed in Supplementary Table S1). These 51 genes were selected on the basis of their association with the enriched biological themes, upregulation of phosphorylation/protein levels in a docetaxel-resistant PC3 model compared to docetaxel-sensitive PC3 (Supplementary Table S2)²², or significant downregulation of transcripts by the mimics. Interestingly, one of these genes is PLK1, whose knockdown is known to be lethal and hence its siRNA is commonly used as a positive control of transfection and in our microRNA screen.

SiRNA knockdown of four genes resulted in significant toxicity – PLK1, FBXO5 (F-box protein 5), TUBA1A (tubulin alpha 1a), RPLP0 (ribosomal protein lateral stalk subunit P0) (Fig. 3). The viability of cells with knockdown of either of these four genes was 20–40% of that of control (non-targeting siRNA) without taxane treatment, and taxane treatment did not decrease their viability further (Fig. 3).

Twelve genes were taxane sensitizers upon siRNA knockdown, where their knockdown increased docetaxel or cabazitaxel sensitivity without an effect in the absence of the taxanes – e.g. CALM1 (calmodulin 1), TMEM65 (transmembrane protein 65), FBN2 (fibrillin 2) (Fig. 3). However, the taxane sensitization effects exerted by the knockdown of these 12 genes were weaker than that of miR-217 and miR-181b-5p mimics. When compared to taxane-treated control, taxane-treated cells with knockdown of either of these 12 genes had 10–20% lower viability whereas taxane-treated mimic-transfected cells had ~30% lower viability (Fig. 3).

Thirty genes were both toxic and taxane sensitizers upon siRNA knockdown – e.g. ANLN (anillin actin binding protein), PKP4 (plakophilin 4), STX2 (synthaxin 2) (Fig. 3). The knockdown of either of these 30 genes caused various degrees of toxicity which was enhanced by docetaxel or cabazitaxel treatment (Fig. 3).

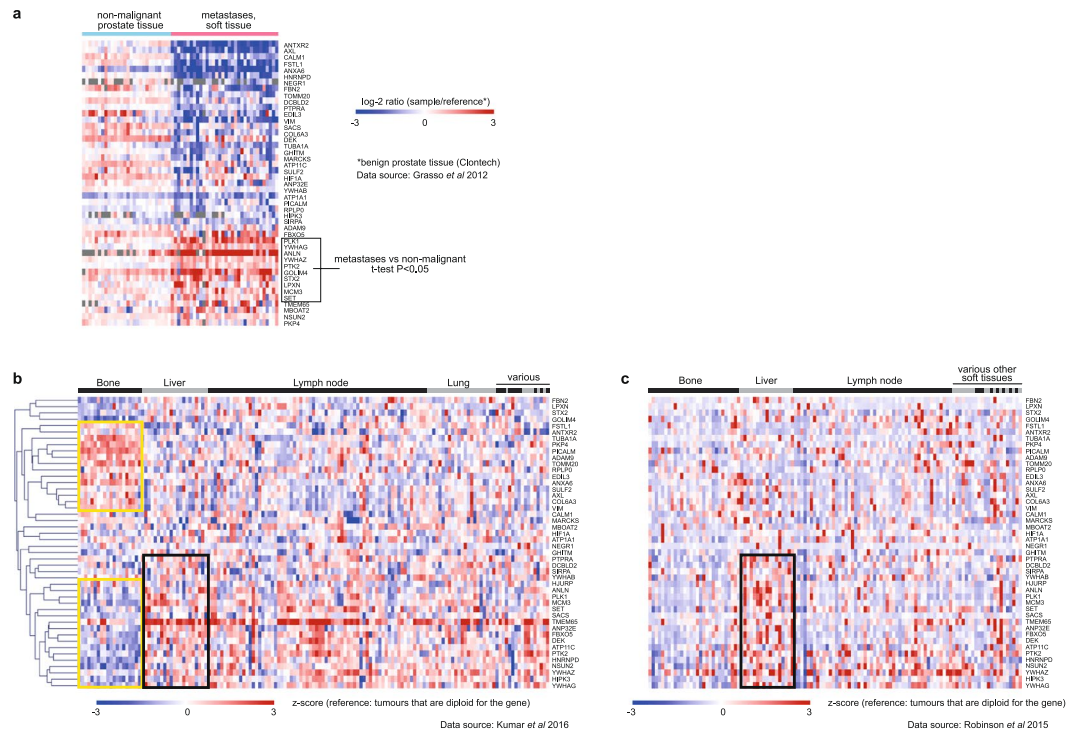


Figure 4. Heatmap of mRNA expression for 46 gene targets of miR-217 or miR-181b-5p mimics in: (a) non-malignant prostate tissue samples from radical prostatectomy of 28 men, and metastatic CRPC samples from rapid autopsy of 34 men; (b) 149 metastatic CRPC samples from rapid autopsy of 63 men; (c) metastatic CRPC biopsies from 118 men. Genes in heatmaps B & C are in the same order.

Overall, a total of 46 genes have toxic (4 genes), taxane sensitisation (12 genes) or both effects (30 genes) when silenced by siRNA knockdown. These 46 genes may be direct or indirect targets of the microRNA mimics that contribute to the taxane sensitisation effect of the mimics. The genes that display toxic effects with or without taxane sensitisation upon siRNA knockdown may be mediating the killing effects of the microRNA mimics in the absence of taxane treatment. Of these 46 genes, 13 were experimentally validated targets of miR-217 or miR-181b-5p according to TarBase version 7 (Fig. 3).

Evaluation of gene targets and microRNAs in genomic tumour datasets. To determine if the genes downregulated by miR-217 and miR-181b-5p mimics in PC3 cells are expressed in human CRPC tumours, the mRNA levels of these genes were examined in three different genomic datasets of CRPC tumours (Grasso *et al.*, Kumar *et al.*, Robinson *et al.*)^{23–25}. The datasets are available from the cBioPortal database²⁶ or NCBI GEO repository. The genes downregulated by the microRNA mimics are referred to as gene targets (direct or indirect) henceforth.

The dataset by Grasso *et al.* consists of 34 CRPC metastases of soft tissue organs obtained at rapid autopsy, and 28 non-malignant prostate tissue samples (unmatched) taken from the radical prostatectomy of patients with prostate cancer²³. Microarray expression data for ~92% of the gene targets of either miR-217 and miR-181b-5p were available for these tissues, of which 18% of miR-217 gene targets and 13% of miR-181b-5p gene targets were significantly upregulated in metastases compared to normal prostate tissue (adjusted t-test P-value ≤ 0.05 , fold ≥ 1.5). Of the 46 gene targets that were shown to have toxic or taxane sensitisation effects upon siRNA knockdown in PC3, ten were upregulated in metastases compared to non-malignant tissues (Fig. 4a). The siRNA knockdown of all these ten genes in PC3 enhanced sensitivity to both docetaxel and cabazitaxel (Fig. 3). Knockdown of all except SET (SET nuclear proto-oncogene) also resulted in toxicity (Fig. 3).

The dataset by Kumar *et al.*²⁴ consists of 129 soft tissue and 20 bone CRPC metastases obtained at rapid autopsy. Non-malignant tissue samples were unavailable for comparison. In this dataset, the gene expression profile of the 46 gene targets in bone metastases differed from that of soft tissue metastases (Fig. 4b). Distinct clusters of genes with increased or decreased expression were evident among the bone metastases, compared to those derived from soft tissue organs (Fig. 4b, outlined in yellow), indicating that the miR-217 and miR-181b-5p mimics may act on different mRNA targets in different metastatic tissues.

Interestingly, the gene expression profile of the 46 gene targets for CRPC metastases in the dataset by Robinson *et al.*²⁵ differed from that of Kumar *et al.* (Fig. 4c). The metastases in the dataset by Robinson *et al.* consists of 89 soft tissue and 29 bone metastases that were obtained by image-guided biopsy from living individuals with CRPC who were being considered for abiraterone or enzalutamide as standard of care²⁵. The distinct cluster of highly expressed genes observed among the bone metastases in the dataset by Kumar *et al.* were not obvious in the dataset by Robinson *et al.* (Fig. 4c). However, a cluster of upregulated genes in liver metastases could be observed in

both datasets (Fig. 4b and c, outlined in black). The variation in the mRNA profile in the dataset by Robinson *et al.* suggests that the miR-217 and miR-181b-5p mimics will have different mRNA targets at different stages of CRPC.

MicroRNA expression data for primary prostate tumours, metastases, and non-malignant prostate tissue, generated by Taylor *et al.* using microarrays²⁷, are available from cBioPortal. The data showed that while miR-181b-5p was detected in both malignant and non-malignant prostate tissues, miR-217 was not (Supplementary Figure S5). Furthermore, miR-217 was not detected in PC3 or DU145 cells, in a previous separate study involving RTPCR analysis of these cell lines using Taqman Array microRNA cards²⁸. The average levels of miR-181b-5p in the metastases from Taylor *et al.*'s dataset was 1.3 fold higher than that of non-malignant prostate tissues (Supplementary Figure S5).

Overall, these genomic data show that the gene targets of miR-217 and miR-181b-5p mimics are expressed in CRPC metastases, indicating that these microRNA mimics may be functional in CRPC. The microRNA mimics are likely to act on different gene targets according to their expression in the metastatic tissues and disease stage.

Discussion

Using a high-throughput genome-wide functional screen, we identified two microRNA mimics – miR-217 and miR-181b-5p, which substantially enhance the docetaxel and cabazitaxel sensitivity of the PC3 prostate cancer cell line. An advantage of utilising microRNA mimics as therapeutic agents is their ability to regulate the expression of multiple genes. It is unclear as to how many and which genes are the key direct targets required to elicit the taxane sensitisation effect of the microRNA mimics, as prediction of direct gene targets is difficult due to imperfect base pairing of microRNAs with their target mRNA. Nevertheless, examination of 46 gene targets with toxic or taxane sensitisation effects showed that these genes are expressed in CRPC metastases. Although the expression profile of these genes vary with metastatic site and disease stage, the ability of microRNAs to affect multiple targets and the presence of more than one gene target in CRPC indicates that these microRNA mimics may be effective in a range of CRPC metastases.

These microRNA mimics appear to enhance the efficacy of the taxanes through mechanisms related to cell proliferation and focal adhesion as these biological themes were enriched among the RNA transcripts downregulated by the microRNA mimics. These mechanisms are consistent with the anti-mitotic and tubulin-targeting action of the taxanes. Taxanes bind directly to microtubules and prevent their disassembly for chromosomal segregation during mitosis, thus resulting in cell cycle arrest in the G2-M phase and induction of apoptosis²⁹. Our study showed that knockdown of genes involved in cell proliferation, which are also targets of the microRNA mimics, resulted in taxane sensitisation or toxicity effects. These genes function as cell-cycle related targets of E2F transcription factors, or are involved in the G2-M phase checkpoint or mitotic spindle assembly. However, differences in cell cycle phases were not observed in cells transfected with the microRNA mimics. This is most likely explained by either (i) modest inhibition of these targets by the microRNA mimics is not sufficient to cause cell cycle arrest, or (ii) the disruption to the cell division process caused by the downregulation of these genes resulted in the cells undergoing apoptosis rather than cell division, as reflected by the observed increase in apoptosis. Interestingly, some of these genes are known to be over-expressed in cancer or associated with poor prognosis such as PLK1, ANLN and FBXO5^{30–32}. Indeed, we observed that both PLK1 and ANLN were significantly upregulated in CRPC metastases compared to non-malignant prostate tissue in the genomic dataset by Grasso *et al.*

Other studies have shown that PLK1 promotes resistance to various chemotherapy agents including docetaxel³³. Presumably PLK1 caused docetaxel resistance by interfering with docetaxel's effect on microtubule dynamics, which also affects androgen signalling in prostate cancer³⁴. Clinical trials of early PLK1 inhibitors in cancers were disappointing, although the newer inhibitor Volasertib showed encouraging results in combination with cytarabine in leukemia³³, suggesting that PLK1 inhibitors may be more effective in a combination setting. Indeed, a recent study showed that PLK1 inhibition enhanced the efficacy of the PARP inhibitor, Olaparib, in BRCA-mutant CRPC cell lines and xenografts³⁵. Targeting PLK1 via miR-217 or miR-181b mimics is akin to a combination approach as the microRNA mimics target multiple genes, and thus may be more effective than using a single agent PLK1 inhibitor.

Taxanes can also disrupt non-mitotic processes that involve microtubules, such as focal adhesion dynamics³⁶. Previously we found that the phosphorylation and protein levels of focal-adhesion and cytoskeletal-related proteins were altered in docetaxel-resistant PC3 and DU145 prostate cancer cells²². These alterations appear to contribute to docetaxel resistance, as inhibition of the activity of one of these proteins, PTK2 (protein tyrosine kinase 2, also known as focal adhesion kinase), using tyrosine kinase inhibitors overcame docetaxel resistance and enhanced docetaxel efficacy in xenografts and *ex vivo* cultures of patient-derived prostate tumours^{22,37}. In the current study, PTK2 and the other affected focal-adhesion or cytoskeletal-related proteins such as VIM (vimentin) and PKP4 (plakophilin 4) were also targets of the miR-217 or miR-181b-5p mimics, and their knockdown caused toxicity and enhanced taxane sensitivity. Overall, these findings demonstrate that various mechanisms centering on microtubules can influence the activity of taxanes.

The subset of miR-217 and miR-181b-5p gene targets examined in this study display differences in docetaxel and cabazitaxel sensitivity upon siRNA knockdown, supporting the existence of differences in the mechanism of actions between the taxanes despite sharing the same molecular target. Other studies have shown that although both taxanes share similar resistance mechanisms, cabazitaxel also has alternative molecular actions as it is effective in docetaxel-resistant models and an enzalutamide-resistant model that was cross-resistant to docetaxel^{38,39}.

To date, there are no studies of miR-217 in prostate cancer. MicroRNA profiling of CRPC showed that miR-217 was not detected in CRPC²⁷, and previously we found that miR-217 was not expressed in PC3 cells²⁸. Studies of various other cancers showed that miR-217 has tumour suppressor properties as miR-217 overexpression inhibited proliferation and invasion, promoted apoptosis, and suppressed xenograft tumour growth^{40–44}. Overall, the findings from these studies indicate that miR-217 mimic is ideal as an anti-cancer therapy. Furthermore, some of these studies also found that the levels of miR-217 in tumours were lower than normal tissue, or inversely

correlated with tumour stage and survival^{42,45,46}. Lower levels of miR-217 in ovarian tumours and leukemia cells was associated with therapeutic resistance^{47,48}.

In contrast, results were conflicting from studies on the role of miR-181b-5p in various cancers, with miR-181b-5p displaying oncogenic properties in some studies^{49–51}, and acting as a tumour suppressor in others^{52–55}. Only one study of miR-181b-5p in prostate cancer has been reported, where suppression of miR-181b expression in PC3 cells induced apoptosis, and inhibited proliferation and invasion⁵⁶. These findings contradict our results, where we showed that miR-181b-5p mimic acted as a tumour suppressor by inhibiting cell growth and enhancing apoptosis.

A limitation of our study is that characterisation of the effects of the microRNA mimics were performed on a single metastatic cell line, PC3, which is derived from a bone metastasis. Both mimics did not affect the taxane sensitivity of the DU145 cell line which was originally derived from a brain metastasis. Nevertheless, brain metastases are quite rare for prostate cancer, where bone is the predominant metastatic site. Of the combined total of 356 metastatic tissues studied by Grasso *et al.*, Kumar *et al.* and Robinson *et al.*, where only 301 specimens have mRNA data as shown in Fig. 4, only two specimens came from the dura. Further studies are required to study the efficacy of microRNA mimics *in vivo* and on various metastases.

Hypothetically, the combination treatment of the microRNA mimics with taxanes would be most effective in tumours with low expression of the microRNAs. Prostate cancer cells do not appear to express miR-217 thus its mimic is likely to be quite effective. MiR-181b-5p is detected in prostate cancer cells, thus a higher dose of its mimic is likely to be required for efficacy.

In vivo testing of miR-217 and miR-181b-5p mimics will be required to evaluate their ability to overcome taxane resistance without significant toxicity. The microRNA mimics can be encapsulated in specialised delivery particles labelled with antibodies targeting tumour antigens such as PSMA to enable selective delivery to prostate cancer cells. This approach was demonstrated in the treatment of malignant pleural mesothelioma with TargomiR, which consisted of miR-16 mimics packaged in bacteria-derived nanoparticles labelled with an EGFR-antibody¹⁶. The Phase 1 study showed that the treatment was well-tolerated and associated with tumour response or disease stabilisation¹⁶.

In conclusion, we have identified two microRNA mimics that enhanced the efficacy of docetaxel and cabazitaxel in CRPC *in vitro*. With further research and development, these microRNA mimics may have potential to improve taxane chemotherapy response in CRPC patients.

Methods

Cell lines, microRNA mimics, and drugs. PC3 and DU145 cell lines were purchased from the American Type Culture Collection (Manassas, VA, USA) and cultured in RPMI 1640 with 10% fetal calf serum, 1.3 μ M insulin, and 10 mM HEPES. These cell lines were authenticated by CellBank Australia using Short Tandem Repeat profiling.

MiR-217 and miR-181b mimics (miRIDIAN microRNA mimics), and ON-TARGETplus non-targeting control siRNA SMARTpool were purchased from GE Healthcare Dharmacon. Docetaxel (clinical-grade) was purchased from Sanofi-Aventis, Australia, and prepared according to manufacturer's instruction. Cabazitaxel was provided by Sanofi-Aventis and dissolved in 56% ethanol and 10% polysorbate 80 at 5 mg/ml. Working stocks of both drugs were prepared in phosphate-buffered saline or culture medium.

Functional microRNA screen. High-throughput screens of PC3 and DU145 cells with Dharmacon's miRIDIAN microRNA Mimic and Hairpin Inhibitor libraries (version 16) (GE Healthcare Dharmacon) was performed as described in detail by Nikolic *et al.*¹⁹. Basically, reverse transfection of cells with the libraries was performed in 384-well microplates with DharmaFECT-1 Transfection Reagent. Positive and negative technical controls were included on each library plate, including the ON-TARGETplus non-targeting control siRNA SMARTpool (GE Healthcare Dharmacon) which was used as the control for analysis of the mimics or inhibitors. Culture media was replaced with fresh media at 24 hours post-transfection. Cells were treated with taxanes or vehicle control at 3 days post-transfection – PC3: 20 nM docetaxel or 18 nM cabazitaxel for 72 hours; DU145: 8 nM docetaxel or 4 nM cabazitaxel for 48 hours. Cell viability was assessed with the CellTiter-Glo Luminescent Cell Viability Assay (Promega) at 1:2 dilution. The viability of cells transfected with microRNA mimic or inhibitor was represented by luminescence measurements normalised to those of cells transfected with the non-targeting control of respective drug treatments. MicroRNAs known to be associated with cardiotoxicity⁵⁷ were eliminated from the dataset.

Drug dose response curve. Reverse transfection of PC3 cells with microRNA mimics or non-targeting control was performed in 96-well microplates with 3000 cells and 0.08 μ l of DharmaFECT-1 Transfection Reagent per well. At 24 hours post-transfection, culture medium was replaced with fresh medium. At 2 days post-transfection, cells were treated with a range of docetaxel (2-fold increments up to 150 nM) or cabazitaxel (2-fold increments up to 20 nM) doses for 48 or 72 hours respectively. Cell viability was assessed with alamarBlue Cell Viability assay (Invitrogen, ThermoFisher Scientific) by fluorescence detection according to the manufacturer's instructions.

IncuCyte analysis of cell doubling time. The confluency of cells transfected with the microRNA mimics or non-targeting control in 6-well multiwell plates were measured using IncuCyte ZOOM (Essen BioScience), with only a single technical replicate for each treatment per multiwell plate. Images of the cells were recorded every 2 or 4 hours, and confluency (phase analysis) was estimated using the IncuCyte software. Doubling time was calculated using the formula below, where timepoints A and B were selected from the linear phase of the curve, with B being the later timepoint:

$$\frac{\text{timepoint}_B - \text{timepoint}_A}{\text{Log}_2(\text{confluency at timepoint}_B \div \text{confluency at timepoint}_A)}$$

Flow cytometry analysis of apoptosis and cell cycle. Labelling of apoptotic cells was performed using the Annexin V-FITC Apoptosis Detection Kit (BioVisionResearch Products, USA) according to manufacturer's instructions. Cells were prepared for cell cycle analysis by fixing in 70% ethanol at -20°C , followed by staining with 0.1% propidium iodide (Sigma-Aldrich) and $830\mu\text{g/ml}$ RNase A (Sigma-Aldrich). Flow cytometry analysis was performed on the BD FACS Canto II system (BD Biosciences) using the FACSDiva software version 8. Data was analysed with FlowJo version 7.6.5.

RNA sequencing and analysis. Total RNA was extracted from PC3 cells transfected with microRNA mimics or non-targeting control (4 replicates per treatment) using the Qiagen RNeasy mini kit (Qiagen, Germany) according to manufacturer's instructions. Sequencing libraries were prepared with $1\mu\text{g}$ of intact RNA using the TruSeq Stranded mRNA Sample Preparation kit (Illumina) according to the manufacturer's protocol. Sequencing was performed on the Illumina HiSeq. 2500 (125 bp paired-end reads), with 12 samples multiplexed in one lane at approximately 20 million paired-end reads per sample. Raw reads were firstly assessed by FastQC and FastQ screen, then filtered using FastQ-mct (Github repository). Filtered reads were aligned to the human reference genome GRCh38 using STAR software version 2.4.2⁵⁸. Feature count was obtained using RSEM version 1.2.21q⁵⁹.

Transcripts with significantly different levels between cells transfected with microRNA mimic and those with non-targeting control were identified using EdgeR package version 3.14.0⁶⁰. Significantly different transcripts with extremely low RPKM (reads per kilobase per million) for both non-targeting and mimic-transfected cells (RPKM <1), and low variance among the samples (variance $<$ median variance of non-targeting and mimic-transfected cells) were removed before analysis for significant biological themes. Enriched gene sets were identified using the Molecular Signatures Database (Broad Institute, Harvard, USA)²¹.

siRNA knockdown. High-throughput siRNA knockdown of 51 different genes in PC3 cells was performed in 384 well microplates using the Caliper Zephyr Liquid Handling Workstation (Caliper Life Sciences, USA) and BioTek EL406 microplate dispenser/washer (BioTek Instruments, USA). All siRNAs were from the ON-TARGETplus SMARTpool collection (GE Healthcare Dharmacon). Reverse transfection of PC3 with the siRNAs was performed in the same conditions as for the microRNA screen, with four replicate wells per treatment. At two days post-transfection, culture medium was replaced with fresh medium containing 10 nM docetaxel, 5 nM cabazitaxel or drug-free medium for 72 hours. The miR-217 and miR-181b-5p mimics were included as positive controls. Cell viability was assessed with the CellTiter-Glo Luminescent Cell Viability Assay (Promega, Australia) as for the microRNA screen.

Analysis of gene targets and public datasets. Prediction of microRNA gene targets was performed using our database (<http://microRNA.garvan.unsw.edu.au/mtp/search/index>)¹⁹, which searches and collates the results from five other target prediction databases – StarBase version 2.0, miRTarBase version 4.5, TargetScan version 6.2, miRDB (accessed on April 2013), and DIANA microT-CDS version 5.

Microarray data of mRNA or microRNA expression were obtained from the cBioPortal database²⁶ or NCBI GEO repository. Genes with more than 50% missing values in a tissue set were removed. Missing values were replaced with the minimum value of the dataset. Multiple t-tests were performed in Microsoft Excel (version 14.7.3), with Benjamini-Hochberg adjustment of P-values.

References

- Torre, L. A. *et al.* Global cancer statistics, 2012. *CA Cancer J Clin* **65**, 87–108 (2015).
- Bishr, M. & Saad, F. Overview of the latest treatments for castration-resistant prostate cancer. *Nat Rev Urol* **10**, 522–528 (2013).
- Mateo, J. *et al.* DNA-repair defects and olaparib in metastatic prostate cancer. *N Engl J Med* **373**, 1697–1708 (2015).
- Tannock, I. F. *et al.* Docetaxel plus prednisone or mitoxantrone plus prednisone for advanced prostate cancer. *N Engl J Med* **351**, 1502–1512 (2004).
- Petrylak, D. P. *et al.* Docetaxel and estramustine compared with mitoxantrone and prednisone for advanced refractory prostate cancer. *N Engl J Med* **351**, 1513–1520 (2004).
- James, N. D. *et al.* Addition of docetaxel, zoledronic acid, or both to first-line long-term hormone therapy in prostate cancer (STAMPEDE): survival results from an adaptive, multiarm, multistage, platform randomised controlled trial. *Lancet* **387**, 1163–1177 (2016).
- Sweeney, C. J. *et al.* Chemohormonal therapy in metastatic hormone-sensitive prostate cancer. *N Engl J Med* **373**, 737–746 (2015).
- de Bono, J. S. *et al.* Prednisone plus cabazitaxel or mitoxantrone for metastatic castration-resistant prostate cancer progressing after docetaxel treatment: a randomised open-label trial. *Lancet* **376**, 1147–1154 (2010).
- Oudard, S. *et al.* Cabazitaxel versus docetaxel as first-line therapy for patients with metastatic castration-resistant prostate cancer: a randomized Phase III trial-FIRSTANA. *J Clin Oncol* **35**, 3189–3197 (2017).
- Lujambio, A. & Lowe, S. W. The microcosmos of cancer. *Nature* **482**, 347–355 (2012).
- Landgraf, P. *et al.* A mammalian microRNA expression atlas based on small RNA library sequencing. *Cell* **129**, 1401–1414 (2007).
- Kozomara, A. & Griffiths-Jones, S. miRBase: integrating microRNA annotation and deep-sequencing data. *Nucleic Acids Res* **39**, D152–157 (2011).
- Garzon, R., Marcucci, G. & Croce, C. M. Targeting microRNAs in cancer: rationale, strategies and challenges. *Nat Rev Drug Discov* **9**, 775–789 (2010).
- van Rooij, E. & Kauppinen, S. Development of microRNA therapeutics is coming of age. *EMBO Mol Med* **6**, 851–864 (2014).
- Janssen, H. L. *et al.* Treatment of HCV infection by targeting microRNA. *N Engl J Med* **368**, 1685–1694 (2013).
- van Zandwijk, N. *et al.* Safety and activity of microRNA-loaded minicells in patients with recurrent malignant pleural mesothelioma: a first-in-man, phase 1, open-label, dose-escalation study. *Lancet Oncol* **18**, 1386–1396 (2017).

17. O'Neil, N. J., Bailey, M. L. & Hieter, P. Synthetic lethality and cancer. *Nat Rev Genet* **18**, 613–623 (2017).
18. Lam, L. T. *et al.* A microRNA screen to identify modulators of sensitivity to BCL2 inhibitor ABT-263 (navitoclax). *Mol Cancer Ther* **9**, 2943–2950 (2010).
19. Nikolic, I. *et al.* Discovering cancer vulnerabilities using high-throughput micro-RNA screening. *Nucleic Acids Res* **45**, 12657–12670 (2017).
20. Sethupathy, P., Corda, B. & Hatzigeorgiou, A. G. TarBase: A comprehensive database of experimentally supported animal microRNA targets. *RNA* **12**, 192–197 (2006).
21. Subramanian, A. *et al.* Gene set enrichment analysis: a knowledge-based approach for interpreting genome-wide expression profiles. *Proc Natl Acad Sci USA* **102**, 15545–15550 (2005).
22. Lee, B. Y. *et al.* Phosphoproteomic profiling identifies focal adhesion kinase as a mediator of docetaxel resistance in castrate-resistant prostate cancer. *Mol Cancer Ther* **13**, 190–201 (2014).
23. Grasso, C. S. *et al.* The mutational landscape of lethal castration-resistant prostate cancer. *Nature* **487**, 239–243 (2012).
24. Kumar, A. *et al.* Substantial interindividual and limited intraindividual genomic diversity among tumors from men with metastatic prostate cancer. *Nat Med* **22**, 369–378 (2016).
25. Robinson, D. *et al.* Integrative clinical genomics of advanced prostate cancer. *Cell* **161**, 1215–1228 (2015).
26. Cerami, E. *et al.* The cBio cancer genomics portal: an open platform for exploring multidimensional cancer genomics data. *Cancer Discov* **2**, 401–404 (2012).
27. Taylor, B. S. *et al.* Integrative genomic profiling of human prostate cancer. *Cancer Cell* **18**, 11–22 (2010).
28. Lin, H. M. *et al.* Circulating microRNAs are associated with docetaxel chemotherapy outcome in castration-resistant prostate cancer. *Br J Cancer* **110**, 2462–2471 (2014).
29. Fitzpatrick, J. M. & de Wit, R. Taxane mechanisms of action: potential implications for treatment sequencing in metastatic castration-resistant prostate cancer. *Eur Urol* **65**, 1198–204 (2013).
30. Magnusson, K. *et al.* ANLN is a prognostic biomarker independent of Ki-67 and essential for cell cycle progression in primary breast cancer. *BMC Cancer* **16**, 904 (2016).
31. Vaidyanathan, S. *et al.* *In vivo* overexpression of Emi1 promotes chromosome instability and tumorigenesis. *Oncogene* **35**, 5446–5455 (2016).
32. Weichert, W. *et al.* Polo-like kinase 1 is overexpressed in prostate cancer and linked to higher tumor grades. *Prostate* **60**, 240–245 (2004).
33. Gutteridge, R. E., Ndiaye, M. A., Liu, X. & Ahmad, N. Plk1 Inhibitors in cancer therapy: from laboratory to clinics. *Mol Cancer Ther* **15**, 1427–1435 (2016).
34. Hou, X. *et al.* Plk1-dependent microtubule dynamics promotes androgen receptor signaling in prostate cancer. *Prostate* **73**, 1352–1363 (2013).
35. Li, J. *et al.* Targeting Plk1 to enhance efficacy of olaparib in castration-resistant prostate cancer. *Mol Cancer Ther* **16**, 469–479 (2017).
36. Stehbens, S. & Wittmann, T. Targeting and transport: how microtubules control focal adhesion dynamics. *J Cell Biol* **198**, 481–489 (2012).
37. Lin, H. M. *et al.* Effect of FAK inhibitor VS-6063 (defactinib) on docetaxel efficacy in prostate cancer. *Prostate* **78**, 308–317 (2018).
38. de Leeuw, R. *et al.* Novel actions of next-generation taxanes benefit advanced stages of prostate cancer. *Clin Cancer Res* **21**, 795–807 (2015).
39. van Soest, R. J. *et al.* Targeting the androgen receptor confers *in vivo* cross-resistance between enzalutamide and docetaxel, but not Cabazitaxel, in castration-resistant prostate cancer. *Eur Urol* **67**, 981–985 (2015).
40. Deng, S. *et al.* Chronic pancreatitis and pancreatic cancer demonstrate active epithelial-mesenchymal transition profile, regulated by miR-217-SIRT1 pathway. *Cancer Lett* **355**, 184–191 (2014).
41. Wang, B. *et al.* MicroRNA-217 functions as a prognosis predictor and inhibits colorectal cancer cell proliferation and invasion via an AEG-1 dependent mechanism. *BMC Cancer* **15**, 437 (2015).
42. Zhang, M. *et al.* miR-217 suppresses proliferation, migration, and invasion promoting apoptosis via targeting MTDH in hepatocellular carcinoma. *Oncol Rep* **37**, 1772–1778 (2017).
43. Zhao, W. G. *et al.* The miR-217 microRNA functions as a potential tumor suppressor in pancreatic ductal adenocarcinoma by targeting KRAS. *Carcinogenesis* **31**, 1726–1733 (2010).
44. Li, H. *et al.* MicroRNA-217, down-regulated in clear cell renal cell carcinoma and associated with lower survival, suppresses cell proliferation and migration. *Neoplasia* **60**, 511–515 (2013).
45. Li, J., Li, D. & Zhang, W. Tumor suppressor role of miR-217 in human epithelial ovarian cancer by targeting IGF1R. *Oncol Rep* **35**, 1671–1679 (2016).
46. Wang, H. *et al.* The microRNA-217 functions as a potential tumor suppressor in gastric cancer by targeting GPC5. *PLoS One* **10**, e0125474 (2015).
47. Vecchione, A. *et al.* A microRNA signature defines chemoresistance in ovarian cancer through modulation of angiogenesis. *Proc Natl Acad Sci USA* **110**, 9845–9850 (2013).
48. Nishioka, C. *et al.* Downregulation of miR-217 correlates with resistance of Ph(+) leukemia cells to ABL tyrosine kinase inhibitors. *Cancer Sci* **105**, 297–307 (2014).
49. Brauer-Hartmann, D. *et al.* PML/RAR α -regulated miR-181a/b cluster targets the tumor suppressor RASSF1A in acute promyelocytic leukemia. *Cancer Res* **75**, 3411–3424 (2015).
50. Xia, Y. & Gao, Y. MicroRNA-181b promotes ovarian cancer cell growth and invasion by targeting LATS2. *Biochem Biophys Res Commun* **447**, 446–451 (2014).
51. Yang, L. *et al.* miR-181b promotes cell proliferation and reduces apoptosis by repressing the expression of adenylyl cyclase 9 (AC9) in cervical cancer cells. *FEBS Lett* **588**, 124–130 (2014).
52. Jiang, J. *et al.* Prognostic significance of miR-181b and miR-21 in gastric cancer patients treated with S-1/Oxaliplatin or Doxifluridine/Oxaliplatin. *PLoS One* **6**, e23271 (2011).
53. Li, Z. *et al.* Up-regulation of a HOXA-PBX3 homeobox-gene signature following down-regulation of miR-181 is associated with adverse prognosis in patients with cytogenetically abnormal AML. *Blood* **119**, 2314–2324 (2012).
54. Wang, H. *et al.* Upregulation of miR-181s reverses mesenchymal transition by targeting KPNA4 in glioblastoma. *Sci Rep* **5**, 13072 (2015).
55. Zhao, L. D. *et al.* Epigenetic silencing of miR-181b contributes to tumorigenicity in colorectal cancer by targeting RASSF1A. *Int J Oncol* **48**, 1977–1984 (2016).
56. He, L. *et al.* MicroRNA-181b expression in prostate cancer tissues and its influence on the biological behavior of the prostate cancer cell line PC-3. *Genet Mol Res* **12**, 1012–1021 (2013).
57. Eulalio, A. *et al.* Functional screening identifies miRNAs inducing cardiac regeneration. *Nature* **492**, 376–381 (2012).
58. Dobin, A. *et al.* STAR: ultrafast universal RNA-seq aligner. *Bioinformatics* **29**, 15–21 (2013).
59. Li, B. & Dewey, C. N. RSEM: accurate transcript quantification from RNA-Seq data with or without a reference genome. *BMC Bioinformatics* **12**, 323 (2011).
60. Robinson, M. D., McCarthy, D. J. & Smyth, G. K. edgeR: a Bioconductor package for differential expression analysis of digital gene expression data. *Bioinformatics* **26**, 139–140 (2010).

Acknowledgements

This study was funded by the Prostate Cancer Foundation of Australia (NCG-4212 and Movember Revolutionary Team Award MRTA1), and the Australian Prostate Cancer Research Centre-NSW through funds from the Australian Department of Health. The Victorian Centre for Functional Genomics (K.J.S.) was funded by the Australian Cancer Research Foundation (ACRF), the Victorian Department of Industry, Innovation and Regional Development (DIIRD), the Australian Phenomics Network (APN), and supported by funding from the Australian Government's Education Investment Fund through the Super Science Initiative, the Australasian Genomics Technologies Association (AGTA), the Brockhoff Foundation and the Peter MacCallum Cancer Centre Foundation. A.S. acknowledges the generous support of the McMurtrie family.

Author Contributions

H.M.L. designed and performed experiments, analysed data, and wrote the manuscript; I.N. designed and performed experiments; J.Y., L.C., C.L.C., N.K.Y., C.S. and Z.B. performed experiments; N.D. analysed data; B.E. analysed data and developed the database; E.D. and K.J.S. designed protocols; B.Y.L. and R.J.D. contributed data; L.G.H. supervised the study; A.S. designed and supervised the study.

Additional Information

Supplementary information accompanies this paper at <https://doi.org/10.1038/s41598-018-26050-y>.

Competing Interests: The authors declare no competing interests.

Publisher's note: Springer Nature remains neutral with regard to jurisdictional claims in published maps and institutional affiliations.



Open Access This article is licensed under a Creative Commons Attribution 4.0 International License, which permits use, sharing, adaptation, distribution and reproduction in any medium or format, as long as you give appropriate credit to the original author(s) and the source, provide a link to the Creative Commons license, and indicate if changes were made. The images or other third party material in this article are included in the article's Creative Commons license, unless indicated otherwise in a credit line to the material. If material is not included in the article's Creative Commons license and your intended use is not permitted by statutory regulation or exceeds the permitted use, you will need to obtain permission directly from the copyright holder. To view a copy of this license, visit <http://creativecommons.org/licenses/by/4.0/>.

© The Author(s) 2018